Int. J. Heat Mass Transfer. Vol. 16, pp. 629–640. Pergamon Press 1973. Printed in Great Britain

INFLUENCE OF VARIOUS SURFACE ROUGHNESS ON THE NATURAL CONVECTION

TETSU FUJII and MOTOO FUJII
Research Institute of Industrial Science, Kyushu University, Fukuoka, Japan

and

MASANORI TAKEUCHI
Faculty of Engineering, Fukui University, Fukui, Japan

(*Received* 28 *March* 1972)

Abstract—Experimental results are presented with respect to the influence of various surface roughness on the natural convection of water and spindle oil along a vertical cylinder. Here are introduced the roughness of repeated-ribs of 0·5 mm height and 6·4, 12·8, 25·6 spacing–height ratio, that of dispersed-protrusions of 0·5 mm height, and that of dense-pyramids of 1·0 mm height.

The local heat-transfer coefficients in the turbulent region, which are evaluated based on the base area of the cylinder, increase slightly in the case of water and decrease slightly in the case of oil. The magnitudes of the variations, however, are at most 10 per cent of the values in the case of the smooth surface. The upper limit of the laminar region is also not affected so much by the roughness. Some considerations on these results are presented in reference to the results of measurements made on temperature profiles in the boundary layer and rising velocities of vortex-pairs and turbulent lumps, beside those of observation done on the fluid motion in the boundary layer and those hitherto reported on the case of forced convection.

NOMENCLATURE

Gr_x, local Grashof number;
Gr_x^*, modified local Grashof number $= Gr_x Nu_x$;
h, height of roughness element;
Nu_x, local Nusselt number;
Pr, Prandtl number;
q, heat flux on the base cylindrical surface;
Re, Reynolds number $= ux/\nu_\infty$;
s, spacing of repeated-rib roughness;
t, temperature;
u, velocity of turbulent lump and vortex pair, and maximum velocity in the boundary layer;
x, distance from the leading edge;
y, distance from the heated surface.

Greek symbols
ζ, dimensionless distance from the heated surface $= (y/x)\,Nu_x$
θ, dimensionless temperature $= (t - t_\infty)/(t_0 - t_\infty)$;
ν, kinematic viscosity.

Subscripts
cri, conditions at the upper limit of the laminar region;
l, conditions on the level of the leading edge;
0, conditions on the heated surface;
∞, conditions in the ambient fluid.

1. INTRODUCTION

A HEATED surface practically has more or less natural roughness. Recently, attempts to enhance the heat-transfer coefficient have been made by roughening artificially the heated surface of a heat exchanger. Various experimental studies were made to obtain optimum roughness for the turbulent heat transfer of forced convection in tubes and annuli. They are mainly concerned with the fuel element of a nuclear reactor. Webb *et al.* [1] summarized recent results of these studies. The data also provide us with a clue for forwarding the theoretical studies of the mechanism of the turbulent boundary layer, especially on the characteristics of the turbulent transport process in the close vicinity of the heated surface.

Concerning the influences of the surface roughness on the natural-convection heat transfer, there is only one paper of Prasolov [2] available. In order to clarify the influence of the fouling of boiler tubes upon heat transfer, he measured average heat-transfer coefficients from the outer surface of a horizontal cylinder to air and showed that artificial roughness of pyramid shape of 0·08–0·36 mm height increased the heat-transfer coefficients about 1·5–2 times in the range of Rayleigh number equal to 10^5–3×10^6.

Before now, Fujii *et al.* [3] carried out an experimental study on the natural convection of liquids along a vertical cylinder and found it to be characterized by the following points; the relation between the local heat-transfer coefficient and the flow pattern of the boundary layer, the influence of the conditions of heated surface, i.e. the cases of the uniform heat flux and uniform temperature, the fluctuation of temperature in the boundary layer and the influence of Prandtl number, etc. Recently, several reliable data [4–6] have been reported concerning the turbulent heat transfer in natural convection along a vertical surface. Though the characteristics of these results are qualitatively similar, there are more or less quantitative differences among them. In any case, however, no account was taken for surface roughness.

The aim of the present paper is to clarify the influence of surface roughness on natural-convection heat transfer from a vertical surface to liquids.

2. APPARATUS AND SURFACE ROUGHNESS

The apparatus used was the same as the one described in the previous paper [3], except for the heated surface. Experiments were performed in the order of the cases of repeated-rib, dispersed-protrusion and dense-pyramid roughness.

Figure 1(a) shows a cylinder with repeated-rib roughness. At first, a cylinder with repeated-ribs, whose height h, width b and spacing s were 0·5, 0·5 and 3·2 mm respectively, was machined on a lathe from a smooth brass cylinder of 83 mm o.d., 66 mm i.d. and one meter height. After a series of experiments was carried out for this roughness, the alternative ribs were cut off so that each spacing between the remaining ribs may be 6·4 mm. Finally, experiments were thus performed by using a cylinder with the repeated-ribs of 12·8 mm spacing.

Gomelauri [7] reported about the case of forced convection that the increase of heat-transfer coefficient was maximum when the spacing to height ratio of repeated-rib roughness s/h was equal to 13 and that this result was almost independent of the shape of the rib cross section. The spacings of repeated-rib in the present study were chosen by referring to these results. The height of rib 0·5 mm corresponds to dimensionless distance from the surface $\zeta = 0{\cdot}5$–$0{\cdot}9$, which varies with the heat flux or with the distance from the leading edge, at $Gr_x^* Pr = 4 \times 10^{14}$. According to the measurement of temperature profiles in the turbulent boundary layer along smooth surface, this value of ζ exceeds the dimensionless thickness of the laminar sub-layer. The ribs were, therefore, expected to protrude from the laminar sub-layer, if its thickness suffered no effect from the ribs.

Figure 1(b) shows a cylinder with dispersed-protrusion roughness. It was made from the cylinder with repeated-ribs of 12·8 mm spacing by cutting partially the ribs off so that the remaining protrusions may have about 12·8 mm circumferential distance and about one millimeter circumferential width and distribute in staggered arrangement with respect to the direction of the boundary-layer flow.

Figure 1(c) shows a cylinder with dense-pyramid roughness. It was made from the smooth

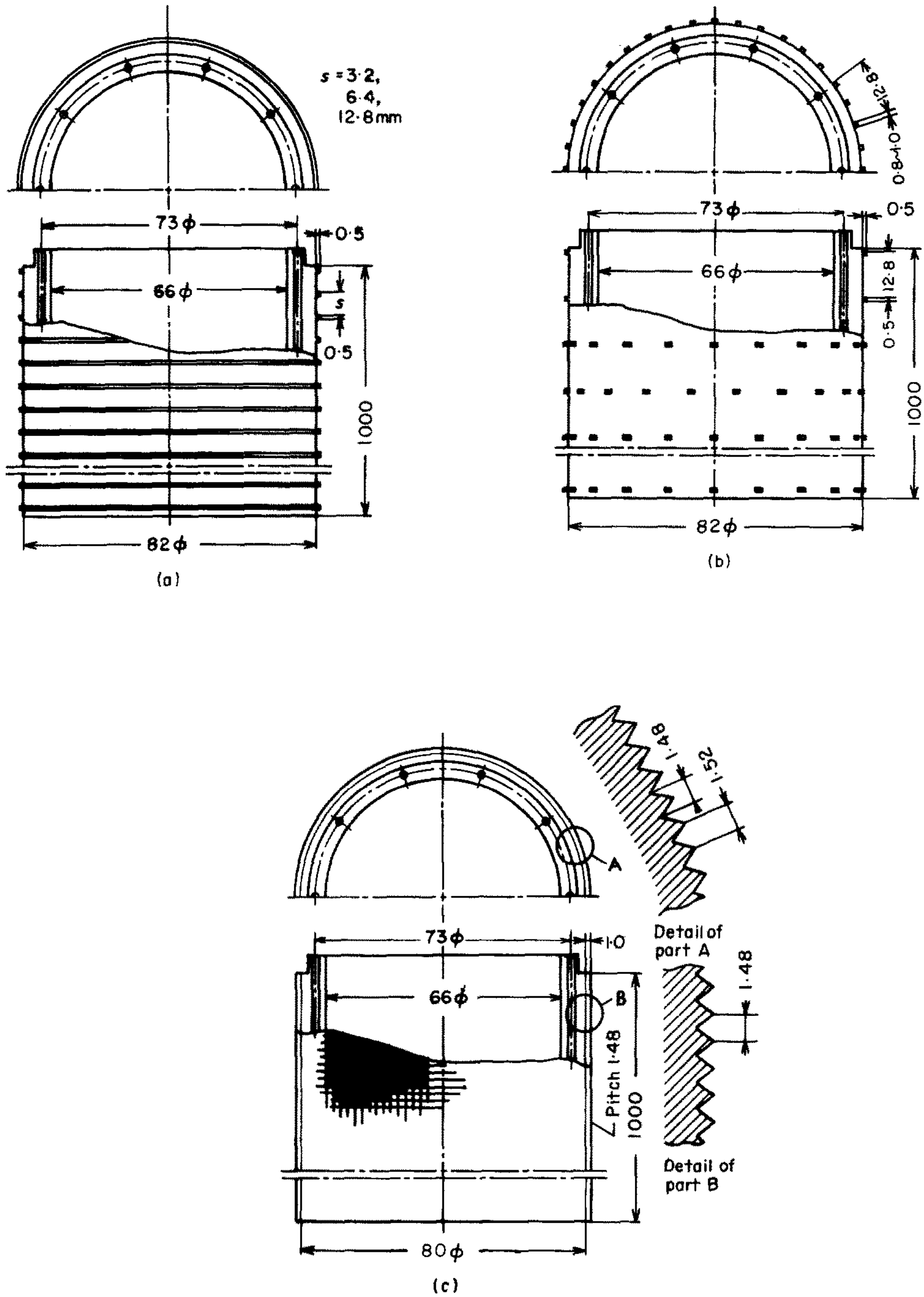

FIG. 1. Shape of surface roughness. (a) Repeated-rib roughness. (b) Dispersed-protrusion roughness. (c) Dense-pyramid roughness.

cylinder of 82·0 mm o.d., which had been made by cutting the protrusions off, by cutting the number of the circumferential and longitudinal triangular groves on the smooth cylinder so that each pyramid formed may have 1·0 mm height and 1·48 by 1·48 mm^2 base area and distribute in in-line arrangement with respect to the direction of the boundary-layer flow. The height of each pyramid was made twice as high as the height of repeated-rib and dispersed-protrusion, because the influences of these roughnesses on heat-transfer coefficients were not remarkable as described later.

The increase of heated-surface area due to the roughness is shown in Table 1 as the ratio to each basic area, which is $0{\cdot}082 \times 3{\cdot}14\ m^2$ for the cylinders with repeated-ribs and dispersed-protrusions and $0{\cdot}080 \times 3{\cdot}14\ m^2$ for the cylinder with dense-pyramids.

3. RESULTS

Only the condition of uniform surface heat flux was chosen for experiments, which was more manageable and yielded more accurate data than that of uniform surface temperature. Besides, in the case of a smooth surface no conspicuous difference was seen between the two conditions about turbulent heat transfer. Dearated pure water and white spindle oil were used for fluids. The ranges of measurements are shown in Table 2. Physical properties in dimensionless numbers are evaluated at the ambient temperature.

3.1 *Local heat-transfer coefficients*

Local heat-transfer coefficients were evaluated based on base cylindrical areas of 82·0 mm dia. for repeated-rib and dispersed-protrusion roughness and of 80·0 mm dia. for dense-pyramid roughness, where no account was taken for the increase of heated-surface area due to roughness. Furthermore, the temperature on the base cylindrical surface above-mentioned was adopted as the representative surface temperature. The values were obtained by setting thermocouples on a cylindrical surface of 73 mm dia. and by correcting the indications of the thermocouples in proportion to the surface heat flux.

Figures 2 and 3 show the relations between $Nu_x(\nu_0/\nu_\infty)^{0\cdot17}$ and Gr_x^*Pr for water and spindle oil respectively, where Nu_x is local Nusselt number, $(\nu_0/\nu_\infty)^{0\cdot17}$ a correction factor for the influence of the variation of viscosity with temperature, Gr_x^* modified local Grashof number and Pr Prandtl number. Solid lines in these

Table 1. Increase of heated surface area

Kinds of roughness	Dense-pyramid	Repeated-rib, s/h = 6·4	12·8	25·6	Dispersed-protrusion
Ratio of real surface area to basic area	1·72	1·32	1·16	1·08	1·01

Table 2. Ranges of measurements

Fluid		Water	Spindle oil
Surface temperature	t_0(°C)	21–92	47–154
Fluid temperature	t_∞(°C)	14–42	15–61
Heat flux	q(W/m^2)	$2{\cdot}5 \times 10^3$–3×10^4	$2{\cdot}5 \times 10^3$–2×10^4
Prandtl number	Pr	4–8	60–260
Modified Grashof number	Gr_x^*	$1{\cdot}5 \times 10^8$–3×10^{14}	$1{\cdot}5 \times 10^7$–4×10^{13}
Modified Rayleigh number	Gr_x^*Pr	1×10^9–1×10^{15}	4×10^9–3×10^{15}
Nusselt number	Nu_x	40–1400	60 × 1900

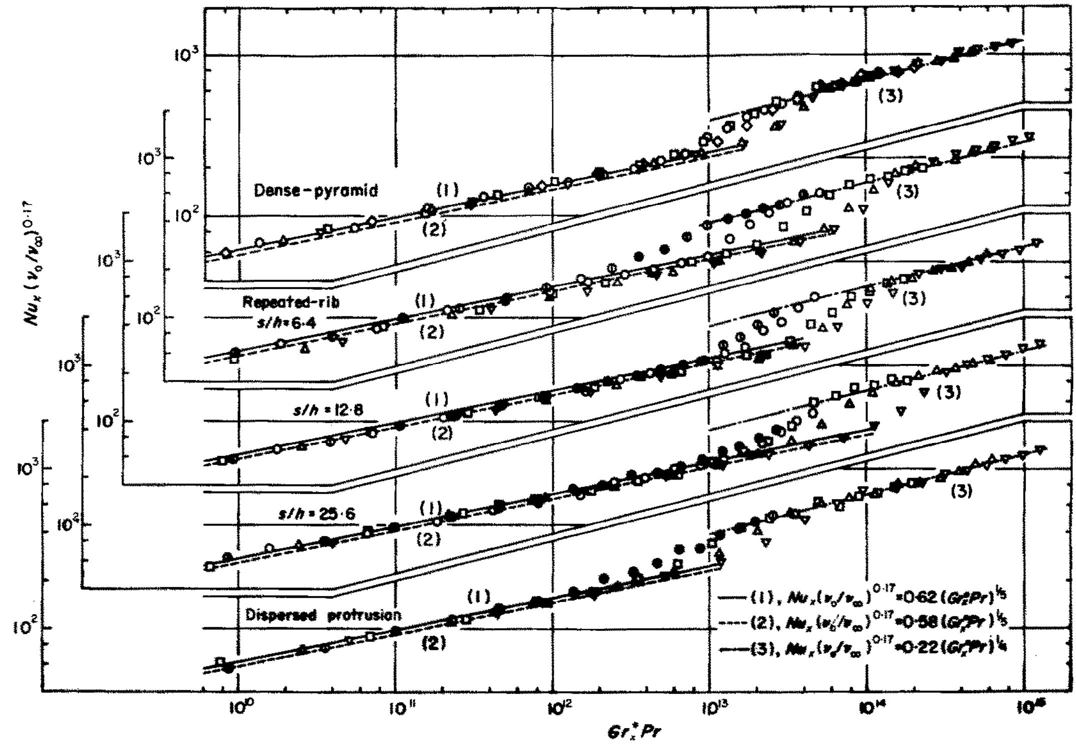

FIG. 2. Dimensionless correlations of local heat transfer coefficients for water.

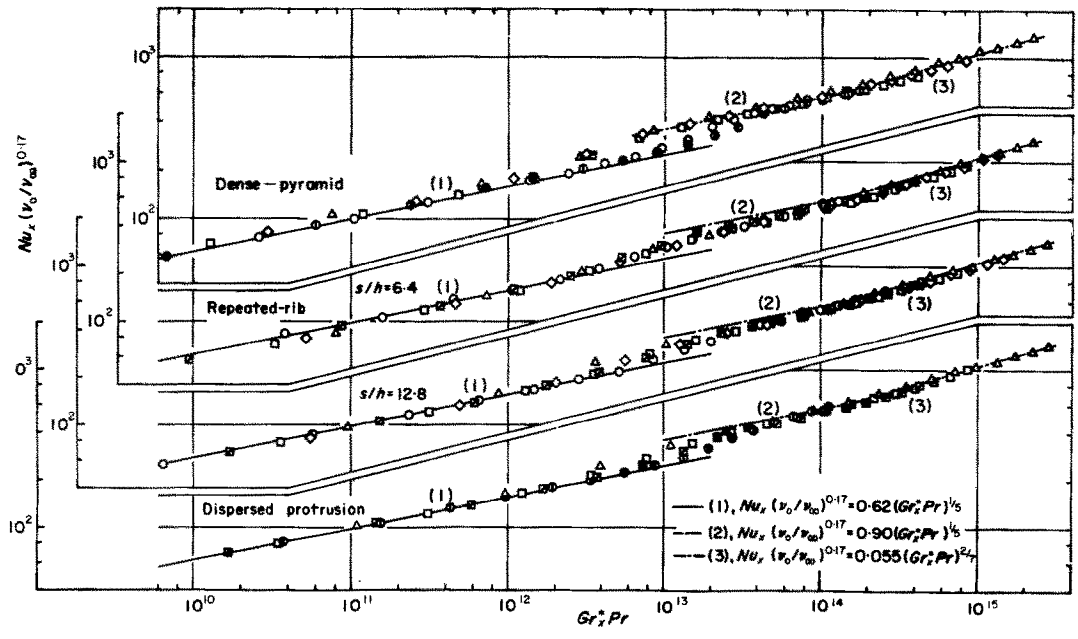

FIG. 3. Dimensionless correlations of local heat transfer coefficients for spindle oil.

figures are correlations of the data for rough surfaces. Broken and chain lines correspond to the theoretical prediction of the laminar region and the experimental expression for the smooth surface proposed in the previous paper [3] respectively.

All of the data in the laminar region are correlated by the expression

$$Nu_x(\nu_0/\nu_\infty)^{0\cdot17} = 0\cdot62(Gr_x^*Pr)^{\frac{1}{5}}, \quad Gr_x^*Pr < 10^{13}. \tag{1}$$

If examined in detail for the data of water, however, there is visible a slight dependence on the type of the surface roughness. When the value of s/h of repeated-rib roughness becomes smaller, the local Nusselt number becomes about 5 per cent lower than the values of expression (1).

When expression (1) is compared with the theoretical prediction in the case of smooth surface, in which the effect of the curvature of cylinder is estimated to be 0·2 per cent at most from [8], the former is about 5 per cent higher than the latter for water of $Pr = 4$–9, whereas both are in good agreement for spindle oil of $Pr = 60$–300.

In the turbulent region for water, the following expression is obtained,

$$Nu_x(\nu_0/\nu_\infty)^{0\cdot17} = 0\cdot22(Gr_x^*Pr)^{\frac{1}{4}}, 10^{13} < Gr_x^*Pr. \tag{2}$$

This expression is quite similar to that for smooth surface. Precisely examined, the local Nusselt numbers for rough surfaces with repeated-ribs of spacing–height ratio of $s/h = 6\cdot4$ and with dense-pyramids are somewhat larger than that of expression (2). The magnitude, however, is about 5 per cent at most.

In the transition–turbulent and turbulent region for spindle oil, the local Nusselt numbers for the smooth surface are expressed as

$$Nu_x(\nu_0/\nu_\infty)^{0\cdot17} = 0\cdot90(Gr_x^*Pr)^{\frac{1}{5}}, \quad 10^{13} < Gr_x^*Pr < 1\cdot5 \times 10^{14} \tag{3}$$

and

$$Nu_x(\nu_0/\nu_\infty)^{0\cdot17} = 0\cdot055(Gr_x^*Pr)^{\frac{2}{7}}, \quad 1\cdot5 \times 10^{14} < Gr_x^*Pr \tag{4}$$

respectively [3]. The data on both dispersed-protrusion and dense-pyramid roughness are in fairly good agreement with these expressions, while the data on repeated-rib roughness are about 10 per cent lower. Furthermore, the transition from laminar region to transition–turbulent region for the roughness of the latter is more gradual than that of the former.

3.2 *Upper limits of the laminar region*

The upper limit of the laminar region is determined from the characteristics of local Nusselt number as shown in Figs. 2 and 3, and also from the observation of the boundary-layer flow. Fujii *et al.* [3] pointed out that the critical Rayleigh number corresponding to the limit was significantly affected by the temperature stratification of the ambient fluid. In that case they used the coordinate system of Rayleigh number $(Gr_xPr)_{cri}$ vs.

$$\frac{(t_{\infty cri} - t_{\infty l})}{(t_0 - t_\infty)_{cri}} \frac{1}{x_{cri}}$$

where $(t_{\infty cri} - t_{\infty l})/x_{cri}$ is the average ambient-temperature gradient from the leading edge to the height x_{cri}, which is corresponding to the upper limit of laminar boundary layer, and $(t_0 - t_\infty)_{cri}$ is the temperature difference between the surface and the ambient fluid at the height x_{cri}.

In this paper, it was to prove how surface roughness effects the critical Rayleigh number that the same coordinate system was used. In Figs. 4(a) and (b) are employed ordinates $(Gr_x^*Pr)_{cri}$ and $(Gr_xPr)_{cri}$ respectively. The data for the smooth surface in the previous paper [3] are also plotted in these figures, where Gr_x^* and Gr_x are mutually converted by the relation of $Gr_x^* = Gr_xNu_x$. The data of the dispersed-protrusion roughness are plotted with the same symbols as those of the smooth surface, because the characteristics of the heat-transfer coefficients of the former are scarcely different from those of the latter.

In Fig. 4(a) a band bounded by solid and dotted lines represents the range of scattering in the data for smooth surface. The solid lines take the gradient -1, and the dotted lines are drawn by referring to the results of Vliet–Liu [5], which were obtained from the experiment made on the case of extremely small temperature stratification of the ambient water and under the condition of uniform surface heat flux. The uncertainty of the critical Rayleigh number within the band seems to be due to the turbulence in the ambient fluid, the type of temperature stratification and other unknown factors. The band in Fig. 4(b) is converted from that of Fig. 4(a) by the same way as data, and, therefore, the gradient of solid lines in this figure is $-0{\cdot}8$. General characteristics of the data in Fig. 4(a) remain the same as in Fig. 4(b).

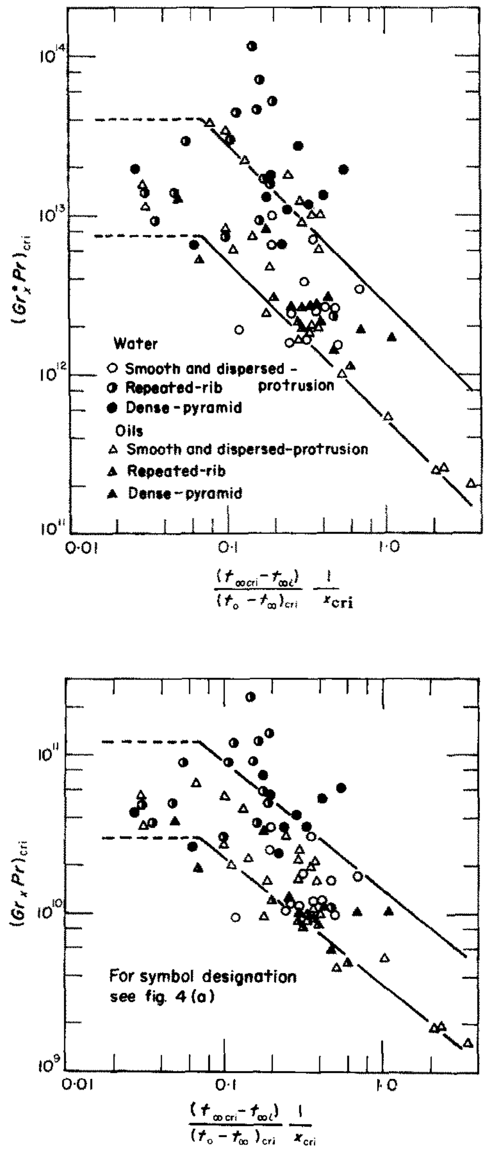

FIG. 4. Upper limits of the laminar region. (a) $(Gr_x^* Pr)_{cri}$ vs. $(t_{\infty cri} - t_{\infty l})/(t_0 - t_\infty)_{cri}/x_{cri}$. (b) $(Gr_x Pr)_{cri}$ vs. $(t_{\infty cri} - t_{\infty l})/(t_0 - t_\infty)_{cri}/x_{cri}$.

Most of the data for spindle oil are not much affected by the surface roughness. In the cases of the repeated-rib and dense-pyramid roughness, some of the data for water are about 3–5 times higher in Rayleigh number than those in the case of the smooth surface.

3.3 *Temperature profiles and flow patterns in the boundary layer*

Temperature profiles in the boundary layer along the vertical cylinder with repeated-rib roughness were measured at two positions, that is, on the planes at mid-height of the width of a rib and at mid-height between two adjacent ribs by using the same apparatus as described in [3]. The profiles of spindle oil for the case of spacing–height ratio of $s/h = 6{\cdot}4$ are shown in Figs. 5(a), (b) and (c), which correspond to the laminar, transition–turbulent and turbulent region respectively. The ordinate of Fig. 5 is dimensionless temperature $\theta = (t - t_\infty)/(t_0 - t_\infty)$ and the abscissa is dimensionless distance from the heated surface $\zeta = (y/x)\,Nu_x$. The local Nusselt number Nu_x in this definition should be evaluated with the local heat flux at the very point where the temperature profile was measured, but there was no other way but to evaluate Nu_x with the average heat flux and representative surface temperature, as defined in 3.1.

The solid lines in Fig. 5(a) are the theoretical predictions for the laminar boundary layer along a smooth surface, and those in Figs. 5(b) and (c) correspond to the experimental expression of

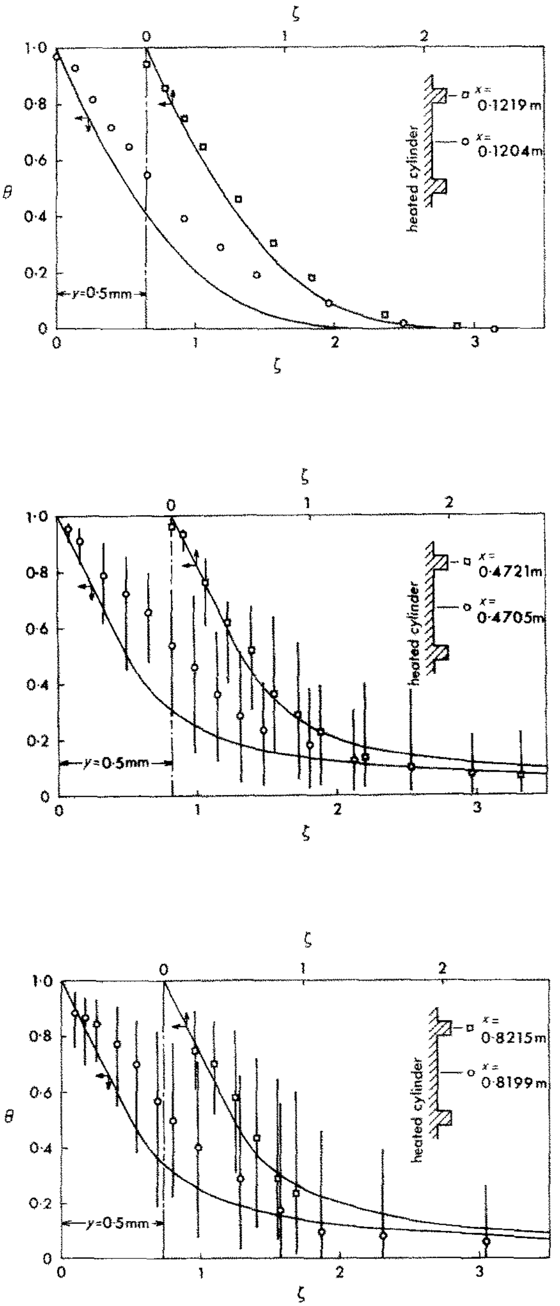

FIG. 5. Time-mean temperature profiles in the boundary layer of spindle oil for the repeated-rib surface of $s/h = 6{\cdot}4$. (a) Laminar region, $Pr = 112$, $Gr_x^*Pr = 3{\cdot}0 \times 10^{11}$ at $x = 0{\cdot}12$ m. (b) Transition–turbulent region. $Pr = 112$. $Gr_x^*Pr = 6{\cdot}9 \times 10^{13}$ at $x = 0{\cdot}47$ m. (c) Turbulent region, $Pr = 109$, $Gr_x^*Pr = 6{\cdot}6 \times 10^{14}$ at $x = 0{\cdot}82$ m.

time–mean temperature profile in the turbulent boundary layer along a smooth vertical cylinder [3]. The vertical bars in the figures indicate the maximum amplitudes of the measured temperature fluctuations. The temperature gradients near the heated surface at the rib agree well with those for the smooth surface, whereas those between the ribs are about 40–50 per cent more gradual than those for the smooth surface. The heat flux, therefore, seems to become dense at ribs and sparse between ribs, though the heat flux supplied from the heater is uniform. For the case of water, the same characteristics as above were also obtained.

It is presumed from the data shown in Fig. 5 that both the laminar boundary layer and the laminar sub-layer of the turbulent boundary layer become thicker as a whole, and, therefore, that the heat-transfer coefficients are probably smaller in comparison to those for the smooth surface. The results in the previous section, however, contradict such a presumption.

Observation of the boundary layer was made by "mirage method" for the most part, as described in detail in [3]. Figure 6 shows mirage photos for the cylinder with repeated-rib roughness of $s/h = 12{\cdot}8$, and (a) and (b) of the figure correspond to the laminar and turbulent region of water and (c), (d) and (e) to the laminar, transition–turbulent and turbulent region of spindle oil respectively. The mirage stripes in the vicinity of the surface are affected by roughness, and those in the boundary layer remote from the surface seem to be similar to those for smooth surface. General tendency of temperature profile, therefore, seems to be in accordance with the results of measurement by thermocouples.

In the laminar region, the stripes above and under the rib are different in shape in the case of water, as shown in Fig. 6(a), but they are symmetrical in the case of spindle oil, as shown in Fig. 6(c). Assuming that the variation of the shape of stripe above the rib represents the flow separation due to the rib, we are convinced that the slight decrease of heat-transfer coefficients is reasonable in the case of water. In the turbulent

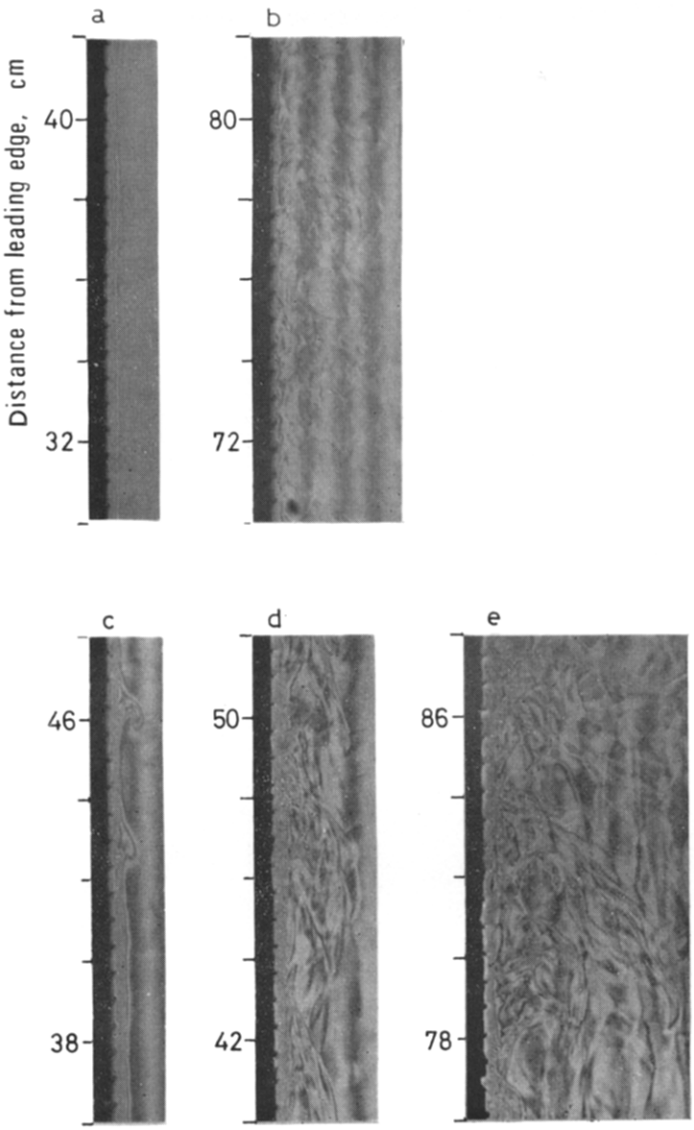

FIG. 6. Flow patterns in the boundary layer along the repeated-rib surface of $s/h = 12{\cdot}8$.

(a) Laminar region of water, $q = 1{\cdot}92 \times 10^4$ W/m^2, $Gr_x^*Pr = 1{\cdot}15 \times 10^{13}$ at $x = 0{\cdot}32$ m.

(b) Turbulent region of water, $q = 1{\cdot}92 \times 10^4$ W/m^2, $Gr_x^*Pr = 2{\cdot}67 \times 10^{14}$ at $x = 0{\cdot}72$ m.

(c) Laminar region of spindle oil, $q = 3{\cdot}2 \times 10^3$ W/m^2, $Gr_x^*Pr = 5{\cdot}19 \times 10^{12}$ at $x = 0{\cdot}37$ m.

(d) Transition–turbulent region of spindle oil, $q = 9{\cdot}5 \times 10^3$ W/m^2, $Gr_x^*Pr = 7{\cdot}64 \times 10^{13}$ at $x = 0{\cdot}47$ m.

(e) Turbulent region of spindle oil, $q = 9{\cdot}5 \times 10^3$ W/m^2, $Gr_x^*Pr = 7{\cdot}37 \times 10^{14}$ at $x = 0{\cdot}82$ m.

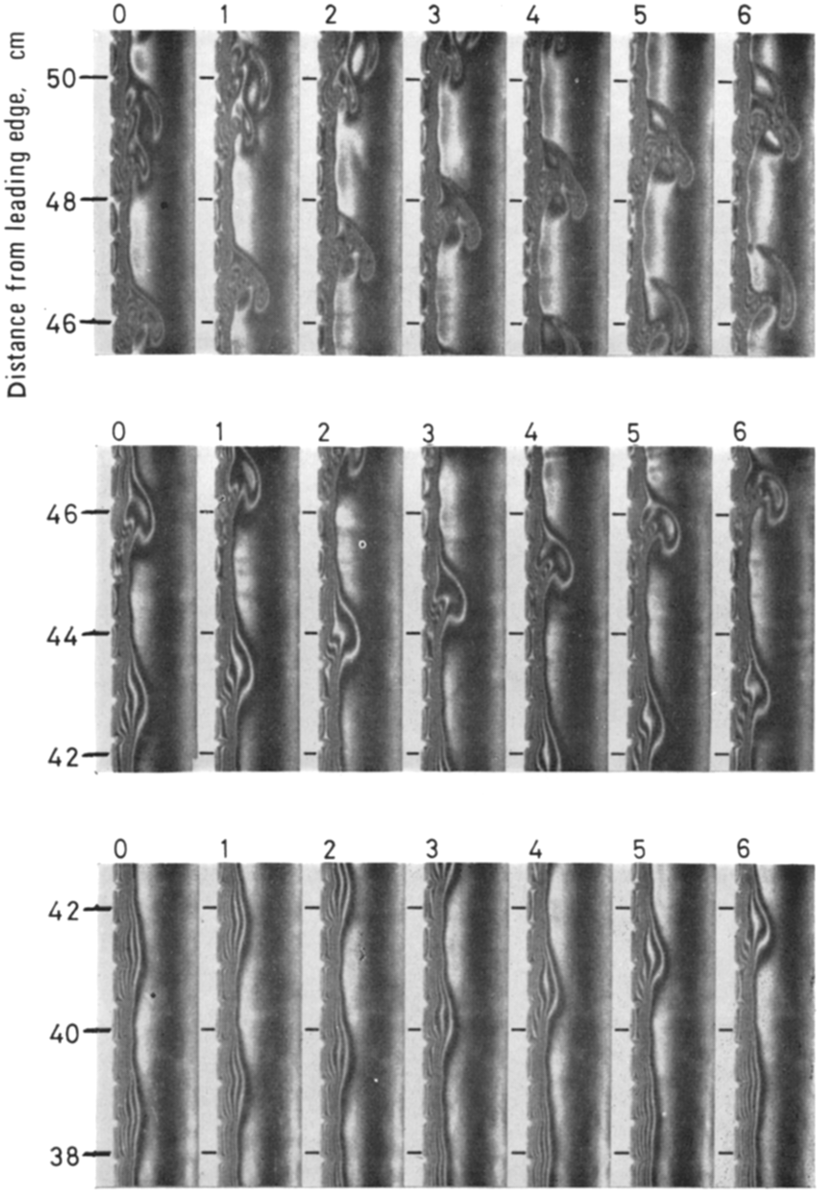

FIG. 7. Development of vortex pairs in the boundary layer of spindle oil for the repeated-rib surface of $s/h = 12{\cdot}8$; $q = 3{\cdot}2 \times 10^3$ W/m², $Gr_x^* Pr = 8{\cdot}65 \times 10^{12}$ and $1{\cdot}37 \times 10^{13}$ at $x = 0{\cdot}42$ and $0{\cdot}47$ m respectively, time interval of each photo is 1/6 s.

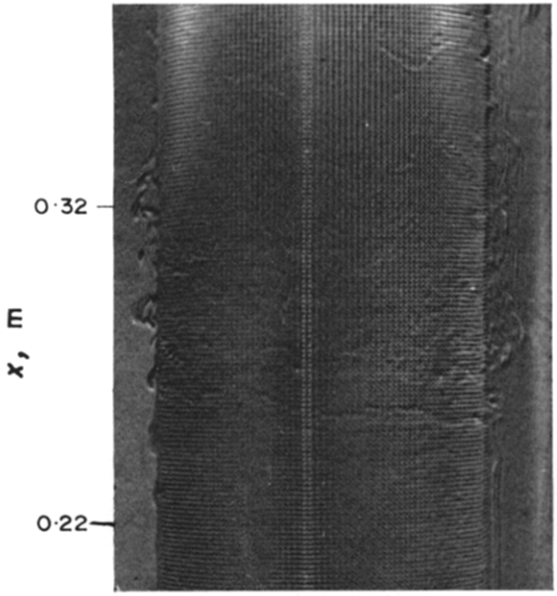

FIG. 8. Front view of the boundary layer of spindle oil in the transition region for the dense-pyramid surface; $q = 1{\cdot}07 \times 10^4$ W/m^2, $Gr_x^* Pr = 3{\cdot}1 \times 10^{12}$ and $1{\cdot}4 \times 10^{13}$ at $x = 0{\cdot}22$ and $0{\cdot}32$ m respectively.

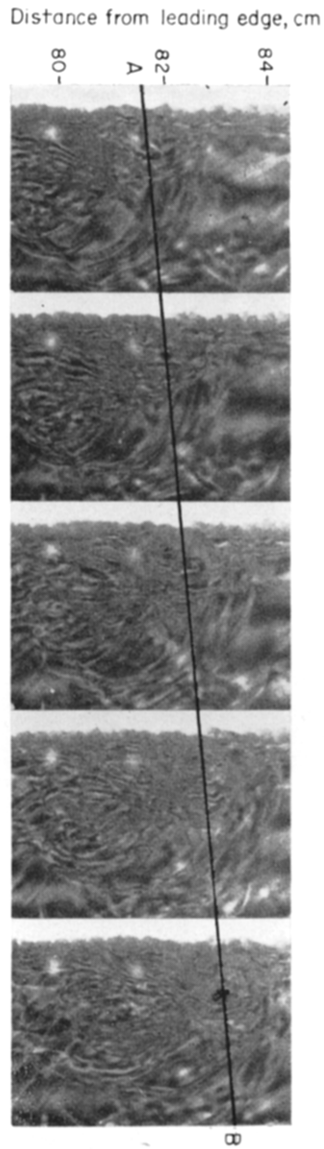

FIG. 9. Turbulent lumps in the boundary layer of spindle oil for the repeated-rib surface of $s/h = 6{\cdot}4$; $q = 1{\cdot}23 \times 10^4$ W/m^2, $ux/\nu_\infty = 8{\cdot}1 \times 10^3$, $Gr_x Pr = 8{\cdot}2 \times 10^{11}$, time interval of each photo is 1/4 s.

and transition–turbulent region, the thickness of laminar sub-layer of water is comparable to the height of rib, as shown in Fig. 6(b), while that of spindle oil seems to become much thicker than this, as shown in Figs. 6(d) and (e). These facts are qualitatively in accordance with the characteristics of heat-transfer coefficient.

A series of mirage photos of Fig. 7 show how the vortex pairs in the boundary layer of spindle oil develop in the case of the repeated-rib roughness of $s/h = 12{\cdot}8$. Despite that the flow near the wall is inevitably affected by ribs, the shape and distribution of the vortex-pairs as well as the period of generation and the ctirical Rayleigh number of transition remain independent of any effect from ribs.

Figure 8 shows a front view of the boundary layer of spindle oil in the transition region from vortex-street to transition–turbulent flow in the case of the dense-pyramid roughness. In this region loops of vortex tubes are formed, as shown in Fig. 18 of [3]. The fact that the loops shown in Fig. 8 do not grow so large as in the case of the smooth surface suggests that the scale of the turbulent mixing becomes smaller and the density of the number of the turbulent lumps becomes larger than those for smooth surface in the transition–turbulent region and the turbulent region formed successively. Such order of variation in turbulent mixing, however, has little influence on the local heat-transfer coefficient.

3.4 *Velocities of vortex-pairs and turbulent lumps*

Rising velocities of vortex-pairs and turbulent lumps are obtained from movie photos. Figure 9 shows an example of successive photos of a turbulent lump of spindle oil, which were taken at the interval of 4/64 s. A straight line AB in the figure is drawn so as to connect a characteristic part of each turbulent lump. From the gradient of line AB the velocity of this turbulent lump is reckoned as $1{\cdot}43/(4/64)/4 = 5{\cdot}7$ cm/s.

The velocities u of vortex-pairs and turbulent lumps thus obtained for the smooth cylinder and the cylinder of repeated-rib roughness are

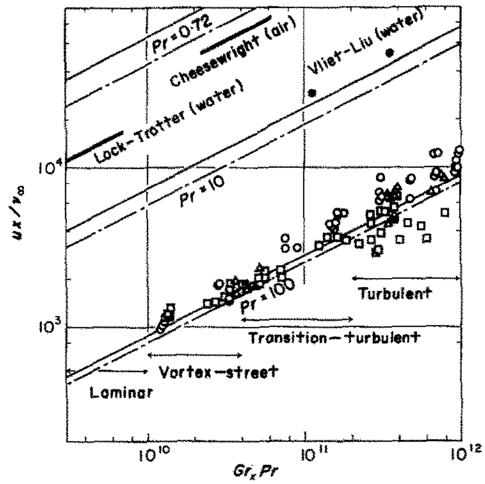

FIG. 10. Rising velocities of vortex pairs and turbulent lumps. ○, smooth; □, repeated-rib $s/h = 12{\cdot}8$; △, repeated-rib $s/h = 6{\cdot}4$; ———, ●, maximum velocity referred from [4, 9, 5]; ———, –·–·–, values at maximum and inflection points of the laminar profiles, which are virtually exterpolated, respectively.

shown in Fig. 10 as the relation between $Re_{x^*} = ux/\nu_\infty$ and $Gr_x Pr$. The solid and chain lines in Fig. 10 show the values at the maximum and inflexion points of the theoretical velocity profiles for the laminar boundary layer respectively, instead of those for the turbulent boundary layer, because there are no reliable theories for it. In Fig. 10 there are also inserted the data on water measured by Vliet–Liu [5] and Lock–Trotter [9] and on air by Cheesewright [4], all of which are corresponding to the maximum values in the turbulent layer.

In the vortex-street and transition–turbulent region shown in Fig. 10, no difference is recognized between the data for the repeated-rib roughness and those for smooth surface, whereas in the turbulent region, the velocities of the turbulent lumps for the rough surfaces are slightly slower than those for the smooth surface. By considering also the facts that the process of the vortex-pair generation is not affected by the surface roughness and that the turbulent lumps are generated as the result of the disintegration of the vortex-pairs, it may be justifiable to presume that the mean velocity in the turbulent boundary layer is nearly independent of the effect also from the surface roughness.

The velocity of the turbulent lumps is almost equal to the maximum velocity of the laminar boundary layer which is virtually exterpolated to the turbulent region. The data on water measured by Vliet–Liu [5] show the same characteristics. The data on water measured by Lock–Trotter [9] are, however, about three times higher and the data on air measured by Cheesewright [4] are about 50 per cent lower in comparison with the virtually exterpolated maximum velocities respectively. Since the turbulent boundary layer carries in it irregular distribution of turbulent lumps with relatively high velocity instead of being homogeneous, the time mean velocity measured is considered to be generally smaller than the velocity of the turbulent lumps. The data of Cheesewright, therefore, seem to be more reasonable than those of Lock–Trotter.

4. CONCLUSIONS AND CONSIDERATIONS

An experimental study was made concerning natural-convection of water and spindle oil along the vertical cylindrical surfaces with three kinds of repeated-rib, dispersed-protrusion and dense-pyramid roughness. The local heat-transfer coefficients, the temperature profiles in the boundary layer and the rising velocities of vortex-pairs and turbulent lumps were measured, and the fluid motion in the boundary layer was observed mainly by means of "mirage method".

Conclusions are as follows;

(1) Practically, it may be appreciated that the surface roughness has little influence on the local heat transfer coefficient, which is evaluated based on the area and temperature of the base surface. The flow patterns in the boundary layer are also not fundamentally altered by the surface roughness.

(2) If examined in detail, a slight variation is recognized. The local Nusselt number for water becomes about 5 per cent lower in the laminar region and about 5 per cent higher in the turbulent region with the increase of the real surface area due to roughness. The local Nusselt number for spindle oil is reduced in the turbulent and transition–turbulent region for repeated-rib roughness, and the magnitude of the reduction is about 10 per cent at most.

(3) The upper limit of the laminar region is generally not affected by the roughness. Some data for water show about 3–5 times higher critical Rayleigh number than that in the case of smooth surface.

Since it is not to be expected to draw above conclusions from the results for the forced convection and from the result of Prasolov [2] for the natural convection, there should be some considerations about their differences.

In the case of forced convection in tubes and annuli, the surface roughness increases the heat-transfer coefficient as well as the friction factor. Kolar [10] correlated the data on the heat-transfer coefficients in terms of Nusselt number and Reynolds number, which is based on friction velocity and tube diameter. Dipprey–Sabersky [11], Sheriff–Gumley [12] and Webb *et al.* [1] used a dimensionless height of roughness, in which usual Reynolds number and friction factor are included. One of the essential results of their studies is that the heat-transfer coefficient is determined by pressure drop independently of the surface roughness. Considering that the driving force in the forced flow corresponds to the pressure drop and that in the natural convection corresponds to the Grashof number, we can analogize that the heat-transfer coefficient in the latter case is not affected by the surface roughness, when compared under the same Grashof number.

The rough surface in the forced convection reduces the mean velocity, and the heat-transfer coefficient is increased just as much as to compensating the loss of the kinetic energy, when compared under the same pressure drop. The mechanism of the increase of heat transfer, such as the separation and the reattachment in the laminar sub-layer, was studied by Edwards–

Sheriff [13], Emerson [14] and Webb *et al.* [1] by using various rib roughness. In the natural convection no remarkable reduction of the mean velocity was measured in the boundary layer along the rough surface, as shown in Fig. 10. Furthermore, there was appreciated no such fact about the laminar sub-layer between ribs becoming thinner than that for the smooth surface, from the temperature profile in the boundary layer. On the other hand, though it is considered that the effective thickness of the laminar sub-layer become rather thicker, the heat-transfer coefficient shows no remarkable reduction. This fact seems to be in common with the fact that the heat-transfer characteristic in the laminar region is scarcely altered. By the way, though plenty of air bubbles are adhered to the heated surface when pure water is used without dearation, the heat-transfer coefficient takes about the same value for dearated water. The quantitative explanation of both these facts and the slight variation of heat-transfer coefficient as described in the second conclusion are left to later survey. Perhaps, microscopic study of the distributions of both surface temperature and heat flux is needed, and the definition of the heat-transfer coefficient must be reconsidered. In that case, the thermal properties of the heated surface will be introduced for a more important role.

Concerning the turbulent flow along the rough plate, Schlichting [15] proposed a admissible height of roughness elements, which caused no increase in drag compared with a smooth surface, namely

$$h_{adm} = 100\nu/U_\infty. \quad (5)$$

In the present experiment, the value of h_{adm} is estimated as about 1 mm for water and as about 8 mm for spindle oil, where the maximum velocities shown in Fig. 10 are used as U_∞ in expression (5). According to above-mentioned analogical inference, the height of the roughness employed in the present experiment may be too small yet, though it is sufficiently high in comparison with the thickness of the laminar sub-layer which is inferred from the temperature profile in the case of the smooth surface.

With regard to the data of Prasolov [2] concerning the average heat-transfer coefficient on horizontal cylinders, we cannot help considering that the saparation of the boundary-layer flow is provoked by the surface roughness. Rayleigh number corresponding to the separation is, however, too small.

ACKNOWLEDGEMENTS

The authors are indebted to Matsunaga Science Foundation for granting them research scholarship on the study of natural convection. Messrs. H. Makino, I. Ishiodori, T. Shigechi, E. Kondoo, M. Furutera, H. Tanaka and M. Izumi assisted in the experiments and the task of manufacturing the apparatus.

REFERENCES

1. R. L. Webb, E. R. G. Eckert and R. J. Goldstein, Heat transfer and friction in tubes with repeated-rib roughness, *Int. J. Heat Mass Transfer* **14**, 601–617 (1971).
2. R. S. Prasolov, On the effects of surface roughness on natural-convection heat transfer from horizontal cylinders to air (in Russian), *Inzh.-Fiz. Zh.* **4**(5), 3–7 (1961).
3. T. Fujii, M. Takeuchi, M. Fujii, K. Suzaki and H. Uehara, Experiment on natural-convection heat transfer from the outer surface of a vertical cylinder to liquids, *Int. J. Heat Mass Transfer* **13**, 753–787 (1970).
4. R. Cheesewright, Turbulent natural convection from a vertical plane surface, *J. Heat Transfer* **90**, 1–8 (1968).
5. G. C. Vliet and C. K. Liu, An experimental study of turbulent natural convection boundary layers, *J. Heat Transfer* **91**, 517–531 (1969).
6. A. Pirovano, S. Viannay and M. Jannot, Convection naturelle en regime turbulent le long d'une plaque plane verticale, *Heat Transfer 1970*, Vol. 4, NC 1. 8. Paris-Versailles (1970).
7. V. Gomelauri, Influence of two-dimensional artificial roughness on convective heat transfer, *Int. J. Heat Mass Transfer* **7**, 653–663 (1964).
8. T. Fujii and H. Uehara, Laminar natural-convective heat transfer from the outer surface of a vertical cylinder, *Int. J. Heat Mass Transfer* **13**, 607–615 (1970).
9. G. S. H. Lock and F. J. de B. Trotter, Observations on the structure of a turbulent free convection boundary layer, *Int. J. Heat Mass Transfer* **11**, 1225–1232 (1968).
10. V. Kolar, Heat transfer in turbulent flow of fluids through smooth and rough tube, *Int. J. Heat Mass Transfer* **8**, 639–653 (1965).
11. D. F. Dipprey and R. H. Sabersky, Heat and momentum transfer in smooth and rough tubes at various Prandtl numbers, *Int. J. Heat Mass Transfer* **6**, 329–353 (1963).

12. N. SHERIFF and P. GUMLEY, Heat-transfer and friction properties of surfaces with discrete roughnesses, *Int. J. Heat Mass Transfer* **9**, 1297–1320 (1966).
13. F. J. EDWARDS and N. SHERIFF, The heat transfer and friction characteristics for forced convection air flow over a particular type of rough surface, *International Development in Heat Transfer*, Colorado U.S.A., pp. 415–425 (1961).
14. W. H. EMERSON, Heat transfer in a duct in regions of separated flow, Proc. Third Int. Heat Transfer Conf. I, Chicago, pp. 267–275 (1966).
15. H. SCHLICHTING, *Boundary-layer Theory*, fourth edition, p. 558. McGraw-Hill, New York (1968).

INFLUENCE DE DIFFERENTES RUGOSITES SUPERFICIELLES SUR LA CONVECTION NATURELLE

Résumé—On présente des résultats expérimentaux concernant l'influence de rugosités superficielles différentes sur la convection naturelle d'eau et d'huile le long d'un cylindre vertical. On a introduit ici la rugosité de canelures répétées hautes de 0,5 mm et de rapport pas/hauteur 6,4, 12,8, 25,6 celle d'excroissances dispersées hautes de 0,5 mm et celle de pyramides serrées de 1 mm de hauteur.

Les coefficients de transfert thermique local dans la région de turbulence, lesquels sont évalués suivant l'aire de la section du cylindre augmentent légèrement dans le cas de l'eau et diminuent légèrement dans le cas de l'huile. Les grandeurs des variations sont cependant de dix pour cent au plus supérieures aux valeurs obtenues dans le cas d'une surface lisse. La limite supérieure de la région laminaire n'est de même pas très affectée par la rugosité. On a présenté quelques considérations sur ces résultats en se référant aux résultats de mesures faites sur des profils de température dans la couche limite et aux vitesses croissantes de paires de tourbillons et masses tourbillonnaires, outre ceux d'observations faites sur le mouvement fluide dans la couche limite et ceux jusqu'à présent rapportés dans le cas de la convection forcée.

EINFLUSS VERSCHIEDENER OBERFLÄCHENRAUHIGKEITEN AUF DEN VORGANG DER FREIEN KONVEKTION

Zusammenfassung—Experimentelle Ergebnisse, die den Einfluss verschiedener Oberflächenrauhigkeiten auf die freie Konvektion von Wasser und Spindelöl entlang eines vertikalen Zylinders zeigen, werden dargestellt. Hier werden Rauhigkeiten eingeführt in Form sich wiederholender Rippen von 0,5 mm Höhe mit einem Abstandsverhältnis von 6,4, 12,8 und 25,6, in Form verstreuter Erhebungen von 0,5 mm Höhe und in Form engliegender Pyramiden von 1,0 mm Höhe.

Der lokale Wärmeübergangskoeffizient im turbulenten Bereich, der berechnet wurde unter Verwendung der Grundfläche des Zylinders, nimmt bei Wasser leicht zu und bei Öl leicht ab. Die Amplituden der Streuung betragen maximal 10% der für den Fall einer glatten Oberfläche sich ergebenden Zahlenwerte. Die obere Grenze des laminaren Bereichs wird also nicht sehr stark durch die Rauhigkeit beeinflusst. Es werden einige Überlegungen zu diesen Ergebnissen angestellt, im Hinblick auf Messungen von Temperaturprofilen in Grenzschichten bei ansteigenden Geschwindigkeiten von Wirbelpaaren und Turbulenzballen, und aufgrund von Beobachtungen der Fluid-Bewegungen in Grenzschichten und—soweit bekannt—für Fälle der erzwungenen Konvektion.

ВЛИЯНИЕ РАЗЛИЧНЫХ ВИДОВ ШЕРОХОВАТОСТИ ПОВЕРХНОСТИ НА ЕСТЕСТВЕННУЮ КОНВЕКЦИЮ

Аннотация—Представлены результаты экспериментального исследования влияния различных видов шероховатости поверхности на естественную конвекцию воды и машинного масла вдоль вертикального цилиндра. Рассматриваются следующие виды шероховатости поверхности: повторяющиеся ребра высотой 0,5 мм с отношением шага к высоте, равным 6,4; 12,8; 25,6, случайно расположенные выступы высотой 0,5 мм и часто расположенные пирамиды высотой 1,0 мм.

Значения локальных коэффициентов теплообмена в турбулентной области, рассчитываемы по площади основания цилиндра, несколько выше для воды и ниже для масла. Однако эти изменения не превышают 10% от значения локального коэффициента теплообмена для гладкой поверхности. Шероховатость не оказывает также большого влияния на верхний предел существования ламинарного режима. Проведено обсуждение таких вопросов как результаты измерения профилей температуры в пограничном слое, возрастания скорости вихревых пар и турбулентных образований. Кроме того, высказаны некоторые соображения отностиельно течения жидкости в пограничном слое и аналогичных результатов по вынужденной конвекции, опубликованных до настоящего времени.